chemosensors

Article

The Usefulness of Autoradiography for DNA Repair Proteins Activity Detection in the Cytoplasm towards Radiolabeled Oligonucleotides Containing 5′,8-Cyclo-2′-deoxyadenosine

Karolina Boguszewska, Bolesław T. Karwowski * and Julia Kaźmierczak-Barańska

DNA Damage Laboratory, Food Science Department, Faculty of Pharmacy, Medical University of Lodz, Ul. Muszynskiego 1, 90-151 Lodz, Poland; karolina.boguszewska@umed.lodz.pl (K.B.); julia.kazmierczak-baranska@umed.lodz.pl (J.K.-B.)
* Correspondence: boleslaw.karwowski@umed.lodz.pl; Tel.: +48-42-677-91-36

Abstract: Autoradiography of ^{32}P-radiolabeled oligonucleotides is one of the most precise detection methods of DNA repair processes. In this study, autoradiography allowed assessing the activity of proteins in the cytoplasm involved in DNA repair. The cytoplasm is the site of protein biosynthesis but is also a target cellular compartment of synthetic therapeutic oligonucleotide (STO) delivery. The DNA-based drugs may be impaired by radiation-induced lesions, such as clustered DNA lesions (CDL) and/or 5′,8-cyclo-2′-deoxypurines (cdPu). CDL and cdPu may appear in the sequence of STO after irradiation and subsequently impair DNA repair, as shown in previous studies. Hence, the interesting questions are (1) is it safe to combine STO treatment with radiotherapy; (2) are repair proteins active in the cytoplasm; and (3) is their activity different in the cytoplasm than in the nucleus? This unique study examined whether the proteins involved in the DNA repair are affected by the CDL while they are still present in the cytoplasm of xrs5, BJ, and XPC cells. Double-stranded oligonucleotides with bi-stranded CDL were used (containing AP site in one strand and a (5′*S*) or (5′*R*) 5′,8-cyclo-2′-deoxyadenosine (cdA) in the other strand located 1 or 4 bp in both directions). The results have shown that the proteins involved in the repair were active in the cytoplasm, but less than in the nucleus. The general trends aligned for cytoplasm and nucleus—lesions located in the 5′-end direction inhibited the course of DNA repair. The combination of STO with radiotherapy should be applied carefully, as unrepaired lesions within STO may impair their therapeutic efficiency.

Keywords: 5′,8-cyclo-2′-deoxyadenosine (cdA); 5′,8-cyclo-2′-deoxypurine (cdPu); nucleic acids; DNA repair; DNA damage; clustered DNA lesions; cytoplasm; therapeutic oligonucleotides; gene therapy; autoradiography

check for updates

Citation: Boguszewska, K.; Karwowski, B.T.; Kaźmierczak-Barańska, J. The Usefulness of Autoradiography for DNA Repair Proteins Activity Detection in the Cytoplasm towards Radiolabeled Oligonucleotides Containing 5′,8-Cyclo-2′-deoxyadenosine. *Chemosensors* **2022**, *10*, 204. https://doi.org/10.3390/chemosensors10060204

Academic Editors: Chaoxing Liu, Michela Alessandra Denti and Hyun Gyu Park

Received: 14 April 2022
Accepted: 26 May 2022
Published: 28 May 2022

1. Introduction

Autoradiography of ^{32}P-radiolabeled material is one of the most precise detection methods of DNA repair processes. The technique has been known for over 70 years in the context of biological applications, such as single-cell analysis [1]. Although it requires specially trained personnel, specialized instruments, and meeting special requirements (which comprise the major limitations of the technique), it remains a low-cost, simple, and highly sensitive detection technique. Thanks to its efficiency, it is commonly used in nucleic acid studies [2–10]. In this study, the autoradiography of ^{32}P-radiolabeled oligonucleotides allowed the detection of changes within oligonucleotides after treatment with cytoplasmic extracts (CE). Samples were radiolabeled (Figure 1A), treated with CE (Figure 1B), and subsequently separated by polyacrylamide gel electrophoresis (PAGE). The results were visualized on the autoradiography film (Figure 1C). Ionizing radiation (IR) emitted during the decay of ^{32}P isotope (here, located on the 5′-end of double-stranded oligonucleotides) interacts with the silver halide grains of the emulsion on the autoradiography film. The visible image with blackened spots is obtained after photographic development [11]. The

spatial distribution and the amount of the radioactivity corresponding to each reaction product were assessed by densitometric analysis (Figure 1C) [12]. This way, the quantitative changes of ^{32}P-5′-end-labeled oligonucleotides after reactions with CE have been detected. Subsequently, the activity of proteins involved in the DNA repair was evaluated based on the quantity of each reaction product (Figure 1C).

IR is one of the most dangerous factors acting upon the DNA molecule. As the base of radiotherapy, it induces complex DNA damage that leads to the death of cancer cells (including clusters containing double-strand breaks (DSB) and non-DSB lesions) [13]. The dose of 4 Gy (considered lethal to humans) generates approximately 5000 base lesions, 5000 single-strand breaks (SSB), 600 cross-links, or 160 DSB per cell per day [14]. The IR may lead, among others, to the 5′,8-cyclo-2′-deoxypurines (cdPus) formation. CdPus, represented in this article by a 5′,8-cyclo-2′-deoxyadenosine (cdA), are bulky structures (Figure 2A) assigned to the group of tandem lesions [15].

CdPus result from the formation of the covalent bond between C5′ and C8. This extra bond stiffens the lesion structure. Subsequently, the rigidity of the neighboring part of the DNA increases, leading to distortion of the double-stranded DNA helix [16]. CdA may appear within clusters with non-DSB lesions resulting from IR action [17]. CdA occurs in two diastereomeric forms—5′*S* and 5′*R* (Figure 2A), which show different biological impacts, as previously described [10,18–24]. The levels of cdA are estimated as 0.01 (5′*R* isomer) and 0.1 (5′*S* isomer) per every 10^6 DNA nucleosides [25].

Moreover, cdPus being part of the clustered DNA lesions (CDL, two or more lesions within 1-2 DNA helical turns) impacts the helix structure and subsequently may impair the repair of accompanying lesions [8,10,16,19,26]. The higher the number of individual lesions accumulated on a small fragment of DNA, the more difficult the DNA repair. Such DNA damage accumulation may lead to mutagenesis, subsequent cell death, or pathological states such as carcinogenesis [27]. To prevent it, DNA repair systems coordinate lesion recognition and removal followed by "rebuilding" DNA fragments to regain the correctness of the genetic information [8,10,18]. The DNA repair proteins are synthesized in the cytoplasm and, under certain conditions, are translocated into the nucleus to repair the DNA in the case of lesion occurrence. The individual non-DSB lesions present within the CDL are usually recognized and removed by base excision repair (BER) or the more complicated nucleotide excision repair (NER) in a certain order to avoid the formation of DSB. For example, AP sites are usually cleaved before base damage when located 5 bp from each other, and the resulting SSB is repaired first [28]. Furthermore, studies have shown that the presence of cdA impacts the action of repair proteins and/or the DNA repair efficiency of the second lesion within the cluster [7,8,10,19,29–33].

CdPus, represented in this study by the cdA, are usually removed from the genome by the NER system (with low efficiency) because no specific glycosylases are known (capable of removing a single lesion via BER) [34]. The "problem" with cdA removal occurs when NER machinery is defective/inactive [21,35–37]. In *Xeroderma Pigmentosum* (XP) patients, the defect in the NER system may lead to DNA damage accumulation (mainly lesions caused by IR), subsequent mutations, cells malfunctioning, and enhanced carcinogenesis [36,38]. New therapeutic approaches to increase radiotherapy efficacy are still needed [13,39]. New-generation drugs are represented by synthetic therapeutic oligonucleotides (STO) such as antisense oligonucleotides (ASO), AsiDNA (Poly(ADP-Ribose) Polymerase (PARP) inhibitor), mRNA, or siRNA, which are designed to play a role in regulating the expression of genes, e.g., related to radioresistance [39–44]. The STO delivery to their biological targets (nuclear or cytoplasmic compartments containing DNA and mRNA, respectively) faces many challenges [42,45]. However, when successfully introduced to the cell, all STO are present in the cytoplasm at some point during their trafficking. All molecules present in the cytoplasm are susceptible to the damaging action of IR. It may subsequently lead to dysfunctions in proteins' biosynthesis and further impact the biological pathways (e.g., DNA repair in the nucleus and/or mitochondria, the action of therapeutics such as

STO) [46,47]. Therefore, it is worth investigating if damaged STO (e.g., by radiation) have a chance to be repaired and act according to its therapeutic purpose.

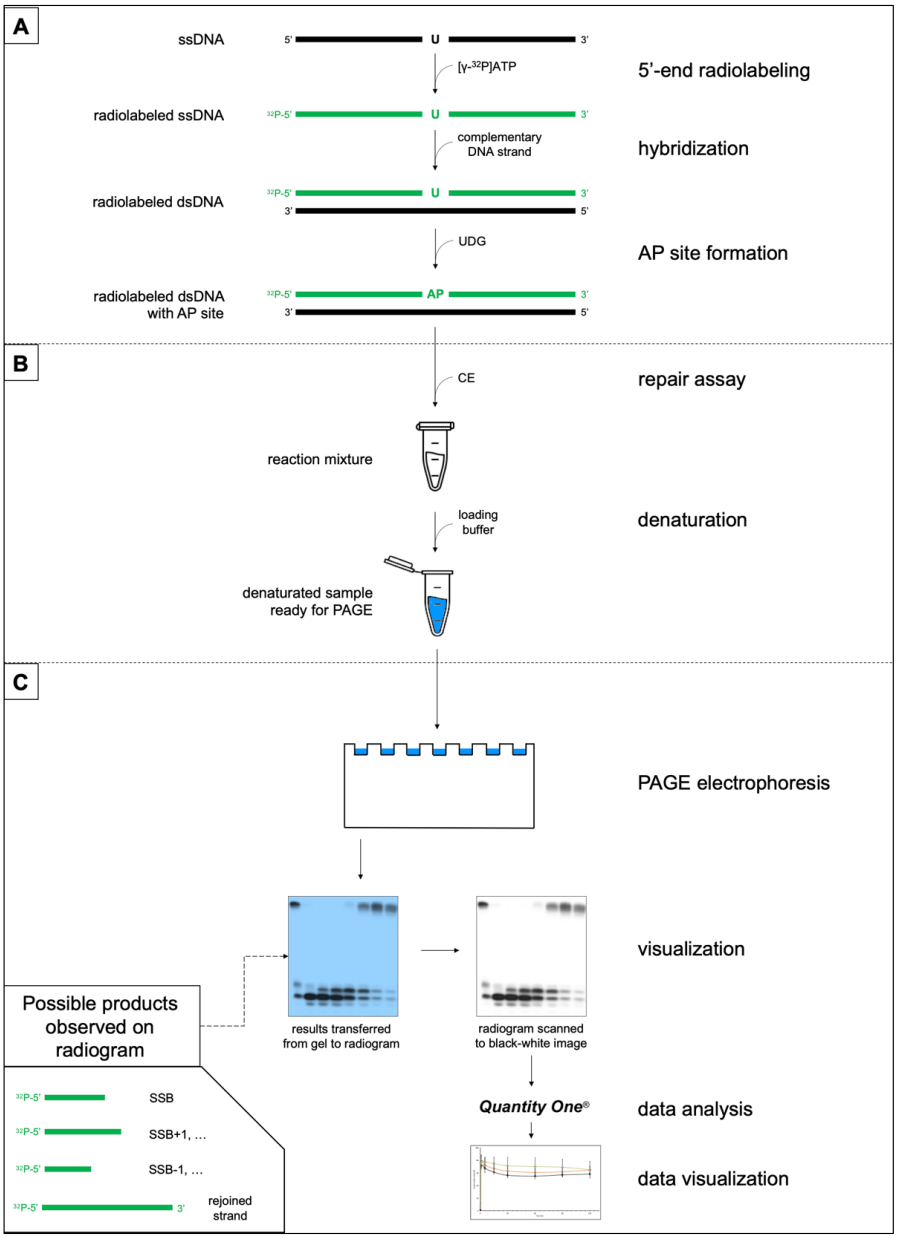

Figure 1. The schematic representation of an experimental procedure used in this study. (**A**) The substrate oligonucleotides' preparation (see Section 2.1). U represents the position of a 2′-deoxyuridine (dU), which served as a precursor of an apurinic/apyrimidinic site (AP site); AP represents the position of an AP site within the strand that was obtained from dU after treatment with uracil DNA-glycosylase (UDG); green color represents a radiolabeled strand of ds-oligonucleotide (40 bp). (**B**) The repair assay experiment (see Section 2.4). Reactions were conducted in 37 °C for 0, 1, 5, 15, 30, 60, 90, and 120 min. The 50 µg of cytoplasmic extracts (CE) was used (see Section 2.3). (**C**) The visualization of obtained results by PAGE, autoradiography, and data analysis. SSB—single-strand break, reaction product obtained after AP site cleavage resulting from the endonucleolytic activity of CE; SSB+1, . . . —reaction products obtained after adding 1 or more nucleotides to the cleaved strand resulting from polymerase activity of CE; SSB−1, . . . —reaction products obtained after removal of 1 or more nucleotides from the cleaved strand resulting from the exonucleolytic activity of CE; and rejoined strand—reaction products obtained after reaching full repair of DNA strand.

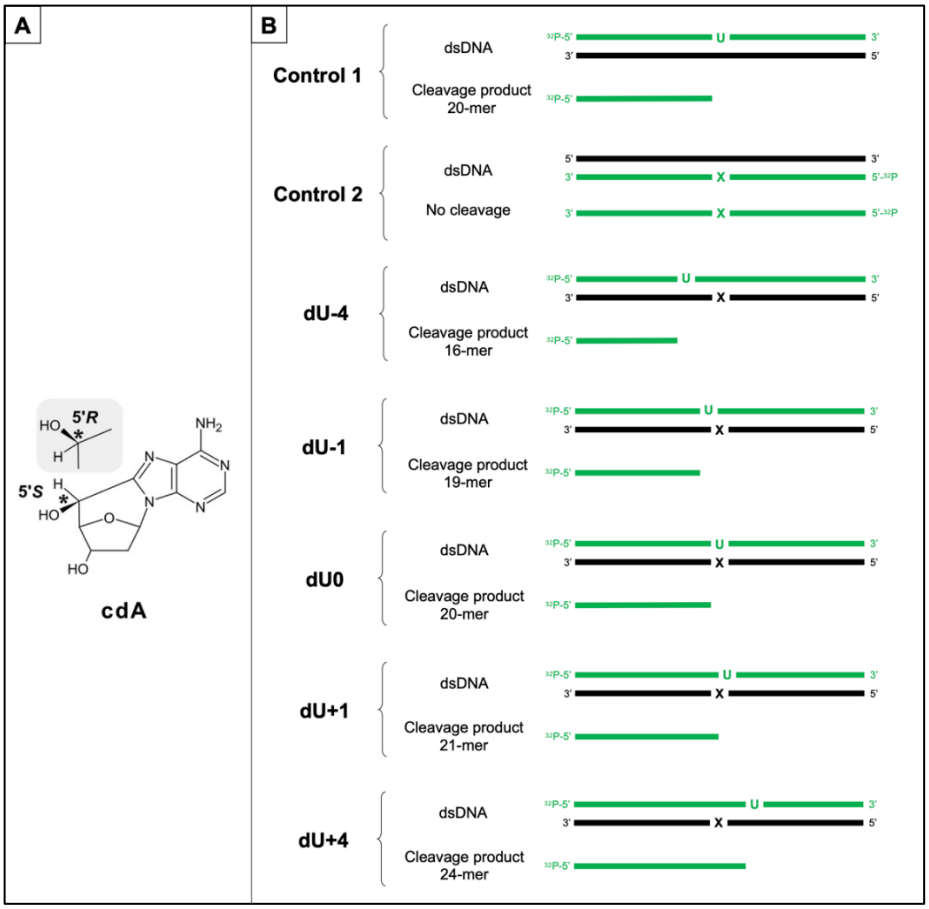

Figure 2. (**A**) The chemical structure of 5′,8-cyclo-2′-deoxyadenosine (cdA) with its 5′*S* and 5′*R* diastereomers. (**B**) The list of investigated double-stranded oligonucleotides. U—the position of an AP site within the strand which was obtained from 2′-deoxyuridine (dU) after treatment with uracil DNA-glycosylase (UDG); X—the position of the cdA within the strand; ^{32}P marks the 5′-end of the strand radiolabeled with [γ-^{32}P]ATP; green color—a radiolabeled strand of ds-oligonucleotides (40 bp) and corresponding cleavage product (observed on autoradiograms; its length depends on the AP site location); negative numbers—ds-oligonucleotides with clustered DNA lesions placed on two strands where AP site is located 1–4 bp in 3′-end direction; positive numbers—ds-oligonucleotides with clustered DNA lesions placed on two strands where AP site is located 1–4 bp in 5′-end direction.

This study mainly considered the safety of combining radiation treatment with therapeutic oligonucleotides applied as a part of gene/anticancer therapy. If the proteins involved in processing/repair of clustered, complex DNA lesions were to be determined as not active in the cytoplasm, the use of STO before cancer cells' irradiation should be carefully considered in the context of other therapeutic schemes. In this scenario, irradiation might damage the STO sequence, which when left unrepaired could give adverse therapeutic effects. This issue has been investigated by (1) testing whether the proteins involved in DNA damage processing/repair were already active in the cytoplasm and (2) assessing the difference between protein activities involved in the DNA damage processing in the cytoplasm and the nucleus. The article describes the complex case of CDL (containing cdA and an AP site), which may be formed as a result of irradiation [26,29,48–50]. This study showed how (5′*S*) and (5′*R*) 5′,8-cyclo-2′-deoxyadenosine affect the repair of clustered DNA damage in the cytoplasm of three cell lines (xrs5, BJ, and XPC). The set of double-stranded 40-mer oligonucleotides containing cdA in one strand and an AP site in the complementary strand at different positions (Figure 2B) was used as an experimental model, and autoradiography was used as a detection technique (Figure 1).

The efficiency of proteins involved in nuclear and mitochondrial DNA repair processes of CDL containing cdPu has been widely studied [6–10,19,30,32,51–55]. Nonetheless, the activity of these proteins was not yet assessed in the cytoplasm. As new therapies arise, specially designed to combine with radiation (such as STO), a detailed understanding of the nature, mechanisms, and implications of the cdA and CDL is especially important.

2. Materials and Methods

2.1. Substrate Oligonucleotides-Containing AP Site

The substrate single-stranded oligonucleotides were synthesized as previously described [56]. The sequences of dsDNA containing cdA in one strand and an AP site in the opposite strand (distanced up to 4 bp in both directions) are presented in Figure 2B and Table S1. Positive numbers (+) were used for dU located in the 5′-end direction and negative numbers (−) were used for dU located in the 3′-end direction from cdA. Substrate oligos were stable in the experimental conditions, as shown previously [8,19]. Moreover, ds-oligos with cdA in their sequence (Control 2) were treated with CE to confirm no additional interactions (Figure S1). Mass spectra of oligonucleotides are presented in Supplementary Materials (Figure S2, Table S2).

The substrate ds-oligonucleotides containing AP sites were prepared as described previously [6–8,10,19,30]. Briefly, ss-oligos were 5′-^{32}P-end-labeled using 2 μCi [γ-^{32}P]ATP (3000 Ci/mmol, 10 mCi/mL, Hartmann Analytic GmbH, Braunschweig, Germany), hybridized with 1.5-fold excess of the complementary strand and treated with 5U of UDG (New England BioLabs, Ipswich, MA, USA). To confirm AP site formation, samples were treated with 5U human apurinic/apyrimidinic endonuclease (hAPE1) (New England BioLabs Ipswich, MA, USA). Each step of the process was verified on 15% native or denaturing polyacrylamide gel (Figure S3). The experimental procedure is shown in Figure 1A.

2.2. Cell Cultures

Three cell lines were investigated: xrs5 (X-ray sensitive Chinese hamster ovarian mutant cell line; used as an established model for in vitro studies on CDL repair), BJ (normal human fibroblasts; used as a reference cell line with unimpaired repair systems), and XPC (fibroblasts obtained from *Xeroderma Pigmentosum* patient complementation group C; used as a model of NER-deficient cells). The xrs5 cell line (CRL-2348, ATCC, VA, USA) was cultured in MEM Alpha (Corning Inc., Corning, NY, USA) supplemented with 10% FBS (Biowest, MO, USA), the BJ cell line (CRL-2522, ATCC, Manassas, VA, USA) was cultured in MEM with Earle's salts and non-essential amino acids supplemented (Gibco, Shanghai, China) with 10% FBS (Biowest LLC, Riverside, MO, USA), and the XPC cell line (GM17420 skin fibroblasts, purchased from the Coriell Institute for Medical Research (Camden, NJ, USA)) was cultured in MEM with Earle's salts and non-essential amino acids (Gibco) and supplemented with 15% FBS (Biowest LLC, Riverside, MO, USA).

2.3. Preparation of Cytoplasmic Extracts

Cells were harvested in the exponential phase, and the CE was obtained using a NE-PER™ Nuclear and Cytoplasmic Extraction Reagents kit (ThermoFisher Scientific, Waltham, MA, USA) according to the manufacturer's instructions. The protein concentration in CE aliquots was tested using colorimetric Pierce™ 660 nm Protein Assay (ThermoFisher Scientific, Waltham, MA, USA) and found between 7.4 and 17.3 mg/mL (xrs5), 7.8 and 21.7 mg/mL (BJ), and 7.4 and 13.6 mg/mL (XPC). Aliquots were stored no longer than 6 months at −80 °C.

2.4. Repair Assays

The substrate ds-oligos (200 CPS) were incubated with 50 μg of CE in the repair buffer (70 mM Tris-HCl (pH 7.5), 5 mM $MgCl_2$, 10 mM DTT, 4 mM ATP, 40 mM PCr, 1.6 μg/mL CK (EC 2.7.3.2), and 0.1 mM of each: dATP, dCTP, dGTP, and dTTP) for 0, 1, 5, 15, 30, 60, 90, and 120 min at 37 °C (Figure 1B). After the required time, a denaturing loading

buffer was added, and samples were examined on a 15% denaturing polyacrylamide gel. Results were visualized by autoradiography (Figure 1C). For consistency, experiments were performed three times. Quantity One software (Bio-Rad, Hercules, CA, USA) was used for data quantification: the processing of AP sites in time was observed on radiograms and expressed as the % of individual bands' intensity (compared to the total intensity of bands for each lane), as described previously [8].

3. Results

The study examined the changes in the activity of proteins involved in DNA damage processing/repair in the cytoplasm of three cell lines (xrs5, BJ, and XPC). The influence of the distance between lesions (cdA and AP site) within CDL was assessed. Moreover, stereoisomers of cdA and their different impacts on protein activity toward the AP site were evaluated.

The synthetic ds-oligonucleotides with AP sites in various positions in one strand and cdA in an opposite strand (ScdA and RcdA) were used as an experimental model (Figure 2, Table S1). Each step of the substrates' preparation was verified: 5′-^{32}P-end-labeling of ss-oligos and hybridization (Figure S3), formation of AP sites (derived from dU after UDG digestion), and subsequent formation of SSBs (derived from AP sites after hAPE1 digestion) (Figure S3). The substrate ds-oligos containing cdA were stable during treatment with cellular extracts and pure glycosylases, as shown previously [7,8,10,18,30]. An additional test was performed to determine the influence of CE; the stability of substrate oligos in experimental conditions was confirmed up to 120 min (Figure S1).

The activity of CE (containing proteins involved in DNA damage processing and repair mechanisms) was verified. The enzymes' activities towards ds-oligonucleotide containing a single AP site (Control 1, Figure 2, Table S1) are presented in Table 1 (endonuclease activity (strand incision, i.e., formation of SSB), polymerase activity (strand elongation, i.e., SSB+1, SSB+2, etc.), and exonuclease activity (strand degradation, i.e., SSB-1, SSB−2, etc.)). The presented values served as a reference activity of CE for further experiments.

Table 1. The enzymatic activities of cytoplasmic extracts for Control 1 oligonucleotide (containing a single AP site). Raw numerical data are presented in Supplementary Materials in Tables S3–S5.

	xrs5 [%]	**BJ [%]**	**XPC [%]**
Endonucleolytic activity (1 min)	71.0	78.73	64.01
Polymerase activity (30 min)	39.19	31.98	35.82
Exonucleolytic activity (120 min)	2.38	4.69	8.89

Double-stranded DNA (40 bp, Figure 2, Table S1) containing a single cdA lesion in one DNA strand and a single AP site in the opposite DNA strand located up to four nucleobases in both 3′-end and 5′-end directions was incubated with CE (50 µg). The relative positions of lesions were chosen for this study as the most problematic ones based on the previous data [5,7,8,10,30]. This work has focused on the observation of the AP site processing (as a lesion accompanying cdA within CDL). The exemplary autoradiogram is shown in Figure 3.

The evaluation included AP site incision efficiency (endonucleolytic activity), subsequent DNA synthesis (polymerase activity), and strand degradation (exonucleolytic activity) by cytoplasmic proteins involved in DNA damage processing/repair and their comparison between cytoplasmic and nuclear extracts of three cell lines: xrs5, BJ, and XPC (numerical data, graphs with SD, and autoradiograms of individual repeats of each experiment are presented in Supplementary Materials).

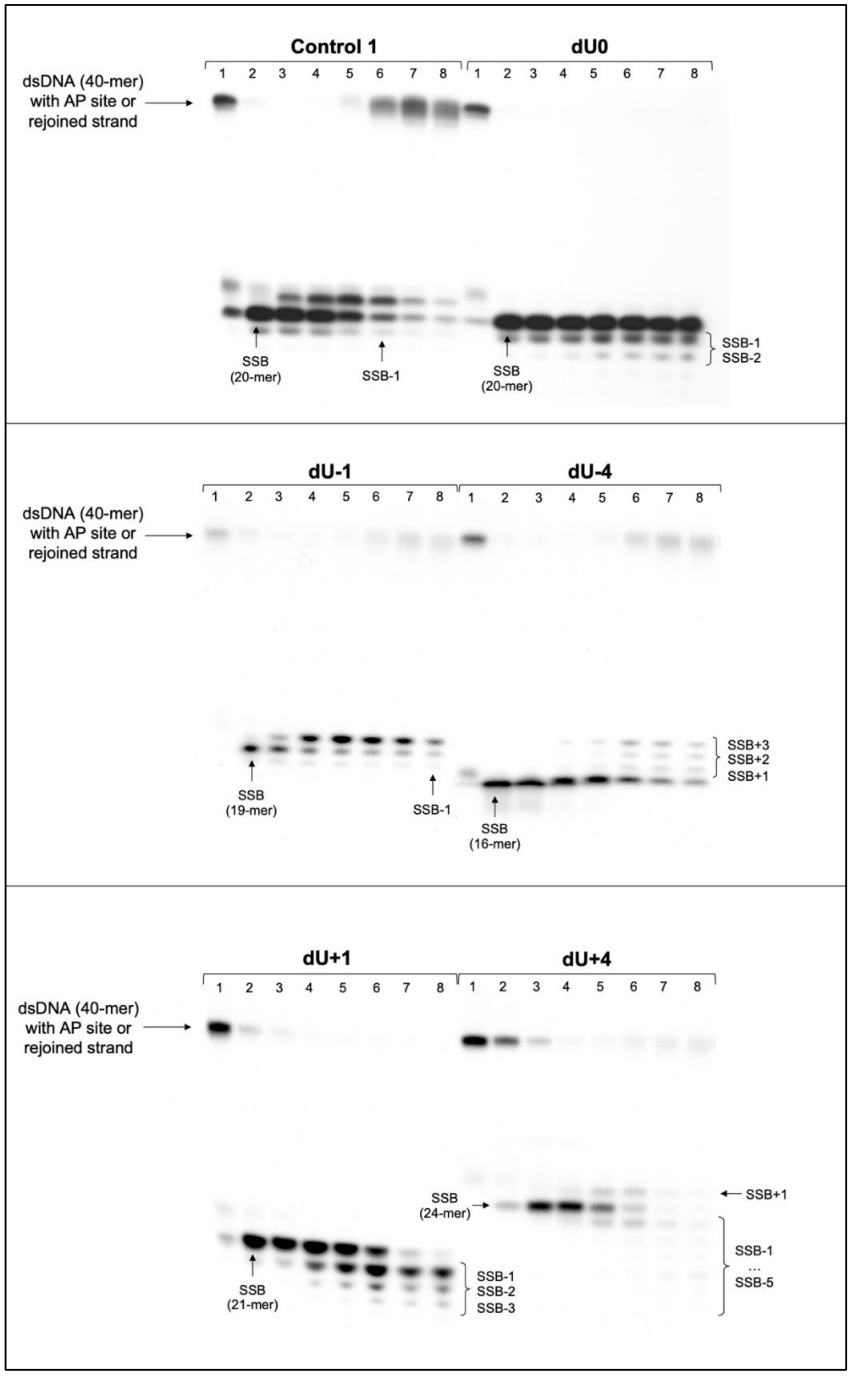

Figure 3. The exemplary autoradiogram of denaturing PAGE (cytoplasmic extract of xrs5 cells). The following protein activities can be observed: the endonucleolytic activity (bands denoted as SSB; dsDNA with single-strand break formed after strand incision by endonucleases), the polymerase activity (bands denoted as SSB+1, SSB+2, etc.; dsDNA with a single-strand break after incorporation of 1 or more undamaged nucleotides by polymerases), and exonucleolytic activity (SSB−1, SSB−2, etc.; dsDNA with a single-strand break after removal of 1 or more nucleotides by exonucleases). In some cases, strand rejoining is also observed, but it is not the focus of this article. Each lane corresponds to a different assay time: lane 1—0 min; lane 2—1 min; lane 3—5 min; lane 4—15 min; lane 5—30 min; lane 6—60 min; lane 7—90 min; and lane 8—120 min. Each experiment was performed three times for results consistency (individual replications, numerical data, and graphical representation of results with SD are available in Supplementary Materials).

3.1. The DNA Strand Incision—Endonucleolytic Activity of Cytoplasmic Extracts

The incision rate at which dsDNA with an AP site in one strand and cdA in the complementary strand was examined. Endonucleases present in CE produce SSB (observed as bands corresponding to 16-mer for −4 position up to 24-mer for +4 position) (Figures 2, 3 and S4–S9).

SSBs were formed for all investigated substrates in all three cell lines after 1 min of incubation with CE (at a minimum rate of ~53%), showing that proteins with endonucleolytic function are active and quite efficient in all tested CE. Exceptions were noted for xrs5 ScdA/dU+4 and RcdA/dU+4, in the cases of which it took 5 min to reach 65.8% and 51.01%, respectively (Tables S6 and S7); also, RcdA/dU+4 in XPC cells increased from 38.54% after 1 min to 86.58% after 5 min (Table S11). Rates for Control 1 ranged from ~64% (XPC) to ~79% (BJ). Incision yields differed depending on the lesion distribution and were increasing in the order presented in Table 2.

Table 2. The general trends of endonucleolytic activity observed after 1 min of reaction time for oligonucleotides containing ds-CDL (shown in Figure 2 and Table S1) treated with cytoplasmic extracts (CE) obtained from three cell lines (raw numerical data is presented in Supplementary Materials in Tables S6–S11) and with nuclear extracts (NE) obtained from three cell lines in previous studies [8,32]. Frames indicate substrates with incision efficiency higher than for corresponding Control 1 (Table 1 and [8,30]).

Strand Incision	xrs5	BJ	XPC
CE	+4 < −1 < +1 < −4 < 0 (ScdA) +4 < −1 < −4 < +1 < 0 (RcdA)	+4 < −1 < 0 < +1 < −4 (ScdA) +4 ~ −1 < +1 < 0 < −4 (RcdA)	−1 < +4 < +1 < 0 < −4 (ScdA) +4 < −1 ~ 0 < +1 < −4 (RcdA)
NE	+4 < −1 < 0 < +1 < −4 (ScdA) +4 < −4 < −1 < +1 < 0 (RcdA)	+4 < −1 < +1 < 0 < −4 (ScdA) +4 < −1 < −4 < +1 < 0 (RcdA)	+4 < −1 < −4 < 0 < +1 (ScdA) +4 < −1 < −4 < +1 < 0 (RcdA)

The lowest endonucleolytic activity was observed for dU+4 in the case of all three cell lines for both diastereomers, which corresponded with the activity noted in previous studies concerning NE (Table 2, Figure 4) [8,30]. In the cytoplasm, the lowest enzymatic efficiency for dU+4 ranged from 39.87% for ScdA in xrs5 to 67.57% for RcdA in BJ (Tables S6–S11).

As described previously, RcdA inhibited endonucleolytic activity in NE more than ScdA [8,30]. This phenomenon seems to align with endonucleolytic activity in CE only for xrs5 and, to some extent, for XPC. Xrs5 cells showed approximately 7–19% lower rates for oligos with RcdA than ScdA (Tables S6 and S7, Figure 4). At the same time, the XPC showed an incision efficiency 11–28% lower for RcdA in the cases of dU0, dU-4, and dU+4, while for dU+1 and dU−1, levels were comparable between isomers (ScdA/dU−1: 58.17%, RcdA/dU−1: 60.64%, ScdA/dU+1: 69.91%, and RcdA/dU+1: 70.52%) (Tables S10 and S11). Interestingly, BJ cells presented the opposite trend. RcdA did not inhibit strand incision but enhanced it by approximately 2–14% (except for dU+1, which showed similar levels of ~77–78% for 5′*S* and 5′*R*) (Tables S8 and S9).

Moreover, only some substrates have shown efficiency rates higher than their corresponding Control 1 level (Tables 1 and 2, Figure 4); for xrs5: ScdA/dU0, RcdA/dU0, and ScdA/dU−4 with a maximum of 79.41%, for BJ: ScdA/dU−4, RcdA/dU−4, and RcdA/dU0 with a maximum of 85.61%; and for XPC: ScdA/dU0, ScdA/dU−4, RcdA/dU−4, ScdA/dU+1, RcdA/dU+1, and ScdA/dU+4 with a maximum of 85.89% (Tables S6–S11).

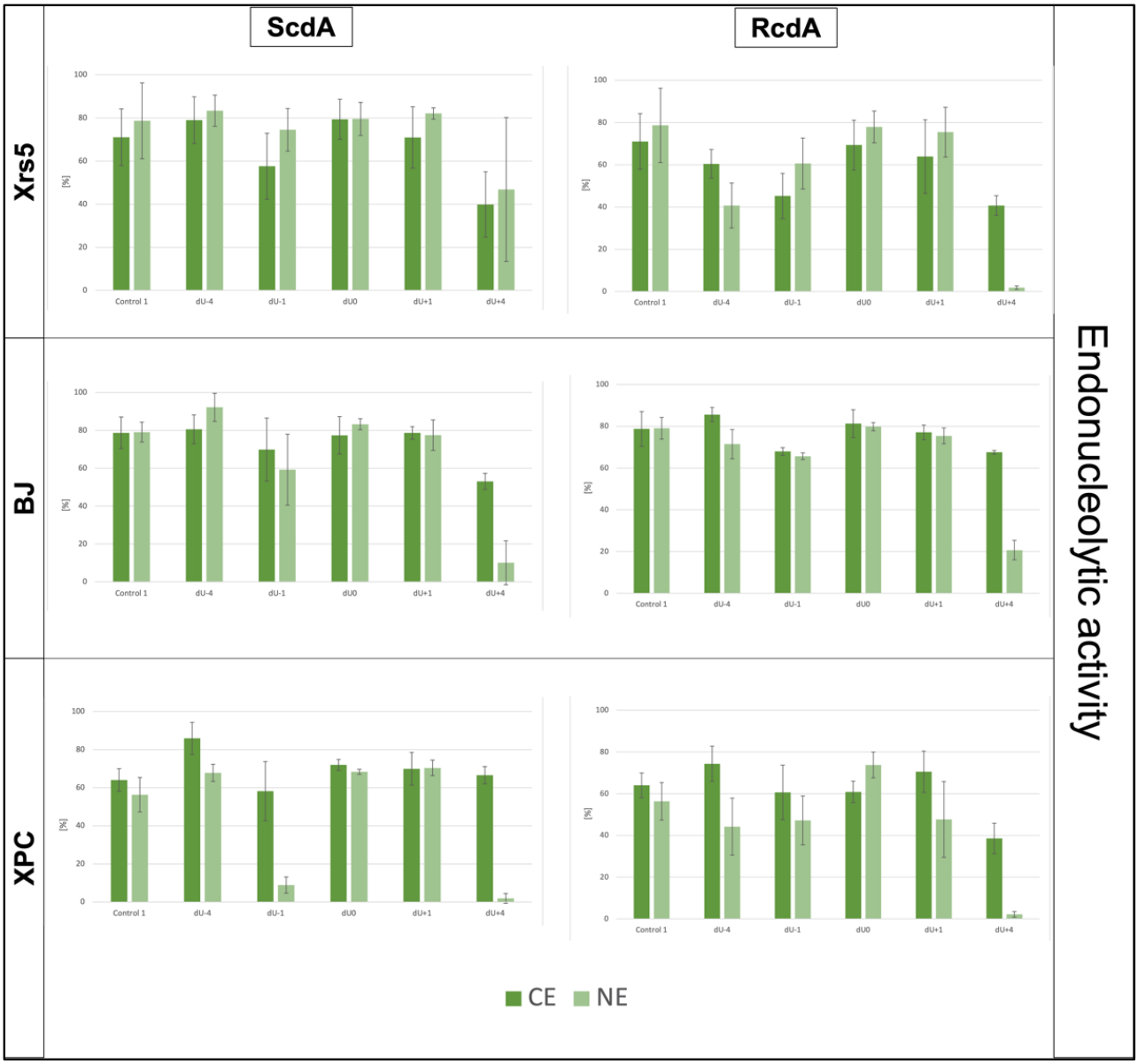

Figure 4. The endonucleolytic activity (observed after 1 min of reaction time) for oligonucleotides containing ds-CDL (shown in Figure 2 and Table S1) treated with cytoplasmic extracts (CE) obtained from three cell lines—xrs5, BJ, and XPC (raw numerical data is presented in Supplementary Materials in Tables S6–S11) and with nuclear extracts (NE) obtained from the same cell lines in previous studies [8,30].

3.2. The DNA Strand Elongation—Polymerase Activity of Cytoplasmic Extracts

The polymerase activity of CE towards oligonucleotides with CDL has also been considered. In all investigated cases, for lesions denoted as dU0 and dU+1, no incorporation of new nucleotides (no SSB+1 bands) was observed, which is consistent with previous studies [7,8,19,30]. Interestingly, the efficiency of DNA strand elongation after 30 min was the lowest (all cell lines, both diastereomers) for dU+4 (13–33%) (Figure 5, Figures S4–S9, S12 and S13, and Tables S6–S11). It was lower than for Control 1 (32–39%) (Table 1). The polymerase activities for the other oligos differed depending on the examined cell line and diastereomeric form of cdA, which is shown in Table 3.

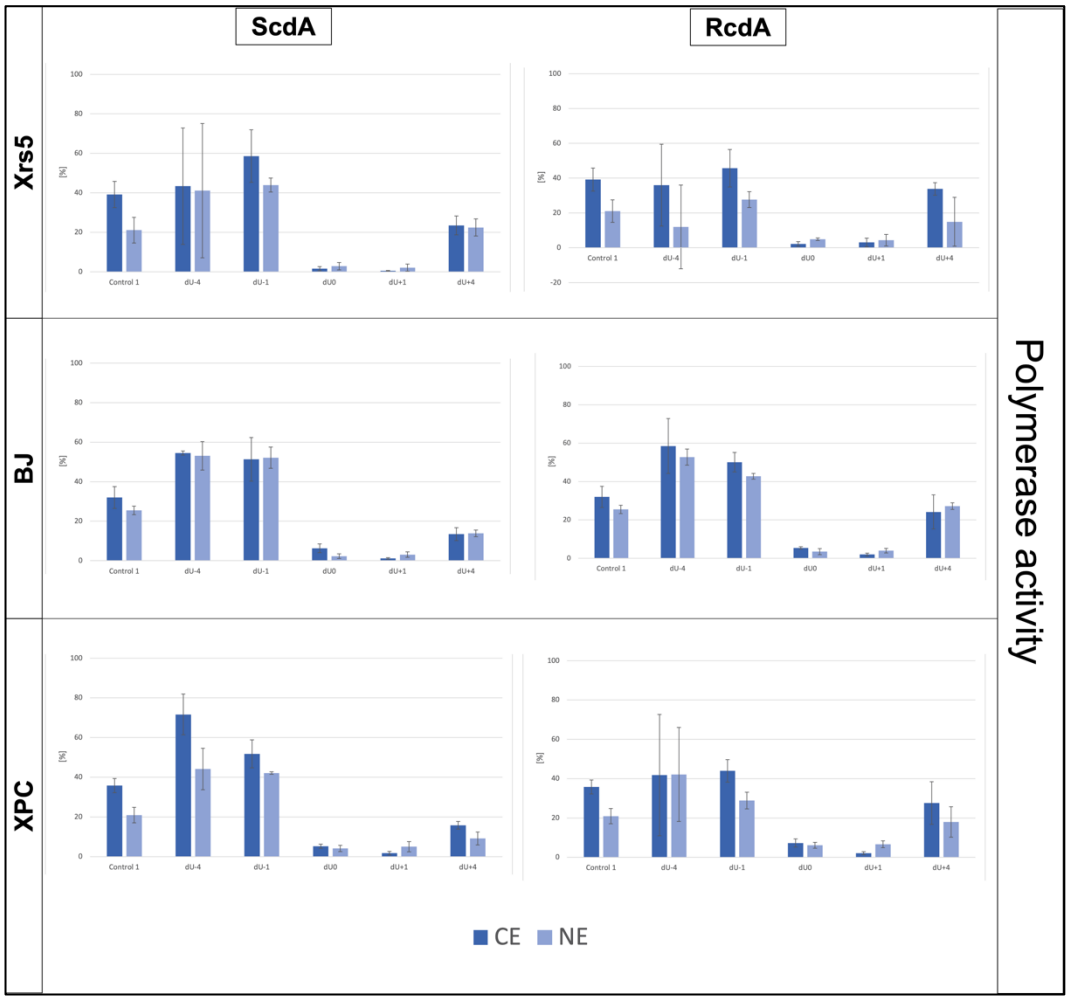

Figure 5. The polymerase activity (observed after 30 min of reaction time) for oligonucleotides containing ds-CDL (shown in Figure 2 and Table S1) treated with cytoplasmic extracts (CE) obtained from three cell lines—xrs5, BJ, and XPC (raw numerical data is presented in Supplementary Materials in Tables S6–S11) and with nuclear extracts (NE) obtained from the same cell lines in previous studies [8,30].

Table 3. The general trends of polymerase activity observed after 30 min of reaction time for oligonucleotides containing ds-CDL (shown in Figure 2 and Table S1) treated with cytoplasmic extracts (CE) obtained from three cell lines (raw numerical data is presented in Supplementary Materials in Tables S6–S11) and with nuclear extracts (NE) obtained from three cell lines in previous studies [8,32]. Frames indicate substrates with elongation efficiency higher than for corresponding Control 1 (Table 1 and [8,30]).

Strand Elongation	xrs5	BJ	XPC
CE	+4 < −4 < −1 (ScdA) +4 < −4 < −1 (RcdA)	+4 < −1 < −4 (ScdA) +4 < −1 < −4 (RcdA)	+4 < −1 < −4 (ScdA) +4 < −4 < −1 (RcdA)
NE	+4 < −4 < −1 (ScdA) −4 < +4 < −1 (RcdA)	+4 < −1 < −4 (ScdA) +4 < −1 < −4 (RcdA)	

The highest activities of polymerases in CE were noted for ScdA/dU−1 (58.63%) and RcdA/dU−1 (45.68%) in xrs5, ScdA/dU−4 (54.53%) and RcdA/dU−4 (58.47%) in BJ, and ScdA/dU−4 (71.65%) and RcdA/dU−1 (44.0%) in XPC (Figure 5, Tables S6–S11). Interestingly, CE presented a common point with previously studied NE. New 2′-deoxynucleotide units (dNUs) were incorporated the most efficiently for 5′*S* and 5′*R* dU−1 in xrs5, for 5′*S*

and 5′*R* dU−4 in BJ, and for 5′*S* and 5′*R* dU−4 in XPC (except for RcdA in CE, where dU−1 showed the highest polymerase activity) (Table 3).

Furthermore, in the NE of xrs5 cells, polymerase activity was 8–20% lower for RcdA than for ScdA, which agreed with the results obtained for the cytoplasm of xrs5: for RcdA/dU−4 and RcdA/dU−1 enzymes were 9% and 13% less active than for 5′*S*, respectively [8]. On the contrary, RcdA/dU+4 showed an approximately 10% higher yield than a corresponding oligo with a 5′*S* isomer (Tables S6 and S7). Experiments involving BJ cells showed different trends in polymerase activity between diastereomers: ScdA/dU+4 was approximately 11% lower than RcdA/dU+4, and ScdA/dU−4 was approximately 4% lower than RcdA/dU−4. Oligo denoted as dU−1 showed a similar yield of strand elongation after 30 min for both isomers (~50–51%) (Tables S8 and S9). Polymerases present in the cytoplasm of the XPC cell line showed the same trends of enzymatic activity as xrs5. Namely, in the case of dU−4 and dU−1, polymerases were 30% and 8% less efficient for RcdA than ScdA, respectively. Moreover, ScdA/dU+4 was elongated with approximately a 12% lower yield than RcdA/dU+4 (Tables S10–S11).

Importantly, the incorporation of more than one dNU was observed for both 5′*S* and 5′*R* isomers; 4 dNUs were added to the DNA strand in positions dU−4 and dU+4 (Figures S4–S9) in all three cell lines. This fact indicates that the LP-BER mechanism may have been involved in these lesion processing in the cytoplasm [55]. It was not observed in past studies for NE or ME obtained from xrs5, nor for NE obtained from BJ and XPC cells [7,8,30]. Interestingly, the polymerase activity of the proteins in CE was similar to or even higher than in the NE (Figure 5), which should be further studied.

3.3. The DNA Strand Degradation—Exonucleolytic Activity of Cytoplasmic Extracts

As expected, exonucleolytic activity was observed in the cytoplasm of all cell lines. Speculations about the trace activity of exonucleases in NE were described in previous studies. These studies concerned the band's intensity loss, which might have resulted from some cross-contamination with cytoplasmic proteins [8]. Here, the strand degradation was evident due to the presence of bands corresponding to SSB−1, SSB−2, etc., on the autoradiograms (Figure 3, Figures S4–S9). Strand degradation was observed for oligos denoted as dU0, dU−1, dU+1, and dU+4 (Figure 3, Figures S4–S9 and S14–S15). Some level of exonucleolytic activity was also noted for Control 1 (less than 10%; Table 1, Figures S4–S9, Tables S3–S5); nonetheless, it was much lower than for investigated oligos in CE from all three cell lines (Tables S6–S11). The efficiency of strand degradation increased in the following order (data compared for 120 min of reaction time) for 5′*S* and 5′*R* isomers of all three cell lines: $-1 < 0 < +4 < +1$ (Tables S6–S11).

The strand degradation rate in the cytoplasm differed between oligos containing the 5′*S* and 5′*R* form of cdA. In xrs5, substrates with ScdA showed approximately 3% lower exonucleolytic activity than RcdA for dU+1 and dU+4 and approximately 7% lower for ScdA/dU−1 and ScdA/dU0 than for corresponding oligos with RcdA (Tables S6–S7). In the case of BJ cells, degradation rate was 4% and 6% lower for RcdA/dU0 and RcdA/dU+4 than for ScdA, respectively. Oligo denoted as dU−1 showed comparable, low degradation rates (~5%), while for dU+1, degradation was approximately 11% higher for 5′*R* than 5′*S* (Tables S8–S10). The CE from XPC cells presented exonucleolytic activity of the 5′*R* isomer higher than 5′*S* for dU0 (53.46% for RcdA/dU0 vs. 37.59% ScdA/dU0) and dU−1 (18.05% for RcdA/dU−1 vs. 9.38% ScdA/dU−1) and lower for dU+1 (88.76% for RcdA/dU+1 vs. 94.95% ScdA/dU+1) and dU+4 (61.05% for RcdA/dU+4 vs. 74.41% ScdA/dU+4) (Tables S10–S11).

What is more, the number of "cut off" dNUs differed depending on the relative position of cdA and a gap/SSB (formed after the AP site's digestion). For xrs5, 2 dNUs were "cut off" in dU0, 1-3 dNUs in dU−1, 4-6 dNUs in dU+4, and 3 dNUs in dU+1 (Figures S4 and S5). For BJ, 2-4 dNUs were released from dU0, 2 or 3 dNUs from dU−1, 6-8 dNUs from dU+4, and 4 dNUs from dU+1 (Figures S6 and S7). For XPC, 3 or 4 dNUs were

removed from dU0, 1-3 dNUs from dU−1, 6 dNUs from dU+4, and 3-5 dNUs from dU+1 (Figures S8 and S9). Control 1 showed a loss of 1 or 2 dNUs in all tested CE (Figures S4–S9).

4. Discussion

Every day, numerous DNA lesions are formed in the human genome because of endogenous (e.g., replication errors, nucleobase modifications, AP site formation) and exogenous (e.g., radiation, chemical agents, environmental stressors) factors [57]. Every hour, approximately 3×10^{17} lesions occur, including the daily formation of 10^4 mutagenic AP sites in each human cell [19,57]. The chemical structures of lesions are the same, irrespectively of their source (endogenous or exogenous). The most endogenously abundant lesions include SSB and AP sites (~600 cell/hour), 8-oxo-dG (~200 cell/hour), thymine glycol (~100 cell/hour) and cytidine deamination products, i.e., dU (192 cell/hour) [58,59]. The situation becomes different when external radiation or chemical factors are introduced (e.g., in the form of chemotherapeutics, radiotherapy, or multimodality treatment [60]). The formation of clustered DNA lesions (DSB and non-DSB) is a characteristic feature of IR's impact on the genetic material. Therefore, proper functioning and survival of the cell depend to a great extent on effective DNA damage processing and repair mechanisms.

The observations presented in this study may find their future application in the fast-growing field of oligonucleotide-based therapies [61–63]. Oligonucleotide-based therapeutics are susceptible to the damaging action of factors such as ROS and IR and may become ineffective after the development of complex lesions in their structures (for example, cdA located within a cluster). Hence, it is worth knowing the consequences of those lesions' occurrence and the mechanisms of their cellular processing. On the other hand, cdPus may be intentionally implemented as a part of oligonucleotide-based drugs/therapies (e.g., to inhibit proteins' action). Therefore, a detailed understanding of cdPus' impact on DNA, DNA damage processing, and DNA repair is highly demanded. Further investigation should take into consideration future therapeutical contexts such as gene therapy, antisense strategies, etc. [43,62].

In this study, for the first time, the cytoplasmic processing of dsDNA with CDL containing cdA has been shown. CdA has two diastereomeric forms (5′*S* and 5′*R*), which may have a different biological impact and occur in DNA in different amounts [10,18–24]. The lesion distribution and diastereomeric form of cdA affect the interaction of enzymes with the other lesion within the cluster (AP site used as a precursor of SSB). The general trends previously denoted for nuclear extracts align with those observed for cytoplasmic extracts derived from the xrs5, BJ, and XPC cell lines [8,30]. Xrs5 was used, as it is an established model for in vitro studies on CDL repair via the BER system; XPC was used as a human model of NER-deficient cells; and BJ was used as a human reference cell line with unimpaired DNA repair systems.

The endonucleases present in the cytoplasmic extracts of examined cell lines effectively incised the AP site in the DNA with bi-stranded CDL containing two lesions (cdA and AP site) located up to four bases in the 5′-end and 3′-end directions from cdA. Interestingly, the strand incision was inhibited for dsDNA with RcdA compared to ScdA for xrs5 and XPC, while in BJ the trend was reversed (Table 2, Figure 4). The overall incision efficiency was similar in the cytoplasmic and nuclear extracts (Table 2, Figure 4) [8,30].

Polymerases are one of the most important elements of complex repair systems in the cell. Nevertheless, the high-fidelity polymerases are not able to bypass the bulk structure of cdPus, which may result in replication blockage [18,64]. In this study of short oligonucleotides with bi-stranded CDL, for gaps located opposite to cdA (position dU0) and in position dU+1, no dNU incorporation was observed (Figures 3 and 4, Figures S4–S9). Hence, polymerases present in the cytoplasm were not able to bypass such clusters. This observation agreed with previous ones concerning nuclear and mitochondrial extracts [7,8,10,32]. The rate of new nucleotide incorporation was higher for dsDNA containing gaps located in the 3′-end direction from cdA (i.e., dU−1 and dU−4). Up to four dNUs have been inserted for oligonucleotides denoted as dU−4 and dU+4 with both isomers of cdA in all investi-

gated cell lines. It may indicate the predominant action of a long-patch repair mechanism, e.g., long-patch BER (LP-BER), during which a fragment of 2–12 nucleotides is excised and replaced with correct nucleobases [65]. Interestingly, in previous studies with nuclear extracts, LP-BER was also observed for xrs5 and XPC cell lines [8,30]. However, it occurred randomly and only two dNUs were incorporated. It may indicate the presence of proteins in the cytoplasm that were not translocated to the nucleus, or it may point to a higher activity of proteins necessary for LP-BER in the cytoplasm, prior to their translocation to the nucleus. This issue would need further and detailed investigation to conclude.

The exonucleolytic activity towards ds-oligonucleotides containing bi-stranded CDL (i.e., cdA and a gap) located up to four bases in 5′-end and 3′-end directions was noted for all investigated CE. It confirms the presence of exonucleolytic proteins in the cytoplasm which are responsible, among others, for the degradation of foreign DNA, and therefore, protection of the cell if such DNA appears (e.g., in case of viral infection). Noteworthy is that the higher the level of degradation, the lower the level of lesion processing or strand reconstitution. For example, the highest level of exonucleolytic activity was noted for substrate oligos denoted as dU+1 (up to five removed bases). This study and past studies have shown that the lesion placed +1 to cdPu was not processed by nuclear or mitochondrial polymerases, so the strand could not be rejoined [7,8,30]. Possibly, in this situation, it was redirected onto the degradation path. On the other hand, oligonucleotides denoted as dU−4 have shown no strand degradation in all tested cytoplasmic extracts, but at the same time, the high activity of polymerases was observed (including the incorporation of more than one dNU). The high efficiency of polymerases was also observed for dU−4 treated with nuclear extracts of xrs5, BJ, and XPC cells [8,30]. Moreover, in nuclear extracts of the xrs5 strand, rejoining took place with high efficiency for oligos containing a lesion placed −4 bp from cdA and 5′,8-cyclo-2′-deoxyguanosine (cdG), regardless of their diastereomeric form [8]. Therefore, the competitive action of proteins responsible for DNA reconstitution and DNA degradation may be assumed. From the practical point of view, in the case of STO containing complex damage resulting from irradiation, the oligonucleotides might be directed for degradation instead of repair if the AP site were in the most problematic positions (i.e., dU+1, dU+4) in relation to cdPu; hence, the therapeutic effect of the STO would be obstructed.

5. Conclusions

In conclusion, the presented study showed that the first steps of effective lesion processing (strand incision and strand elongation) of dsDNA containing bi-stranded CDL (with two lesions: AP site vs. (5′*S*)/(5′*R*)cdA) in the cytoplasm depend on the position and distance between both lesions. The overall activity of proteins involved in DNA damage processing/repair in cytoplasmic extracts from xrs5, BJ, and XPC cells differed between 5′*S* and 5′*R* diastereomers. These observations aligned with the previous studies concerning repair mechanisms in the nucleus [8,30].

This article has shown that proteins involved in DNA damage processing (demonstrating endonucleolytic, exonucleolytic, and polymerase activities) were active in cytoplasmic extracts shortly after their biosynthesis and before translocation into the nucleus. Moreover, 5′*S* and 5′*R* diastereomeric forms of cdA have influenced differently the proteins' enzymatic action. Despite the lower activity of proteins in the cytoplasm than in the nucleus, the general trends aligned with the observations from past studies concerning nuclear and mitochondrial extracts [7,8,10,30]. Moreover, enhanced DNA strand degradation was observed when lesions were located +1 nucleobase from cdA within a cluster. These oligonucleotides were not repaired in CE nor in NE from all tested cell lines, which may indicate the competitive action of repair and degradation machinery (when lesions were too complex for repairing, the cytoplasmic degradation rate increased).

Taking into consideration the presented results, the use of synthetic therapeutic oligonucleotides (STO) as a part of anticancer therapy should be carefully considered. The timing of its administration (before, during, or after radiotherapy) seems to be crucial.

STO with complex and clustered DNA lesions in its structure (such as cdA resulting from radiation) might not be effective (e.g., degraded by the cytoplasmic proteins) or even cause adverse effects (due to the possibility of mutations following impaired repair pathway). The results of this study may shed new light on the activity of proteins involved in the DNA damage processing/repair of complex lesions such as CDL and cdPu. Moreover, this article raises some issues to be considered about therapeutic oligonucleotides as a part of anticancer treatment.

Supplementary Materials: The following supporting information can be downloaded at: https://www.mdpi.com/article/10.3390/chemosensors10060204/s1, Figure S1: The stability of "matrix" oligonucleotides, Figure S2: Mass spectra of substrate oligonucleotides containing cdPu, Figure S3: (A) Verification of radiolabeling of single-stranded (ssDNA) and efficient annealing of double-stranded (dsDNA) oligonucleotides (B) Verification of AP sites' stability/purity and SSBs formation, Figure S4: The autoradiograms presenting results—ScdA by xrs5 Cytoplasmic Extract, S5: The autoradiograms presenting results—RcdA by xrs5 Cytoplasmic Extract, Figure S6: The autoradiograms presenting results—ScdA by BJ Cytoplasmic Extract, S7: The autoradiograms presenting results—RcdA by BJ Cytoplasmic Extract, Figure S8: The autoradiograms presenting results—ScdA by XPC Cytoplasmic Extract, S9: The autoradiograms presenting results—RcdA by XPC Cytoplasmic Extract, Figure S10: Endonucleolytic activity of xrs5 vs. BJ vs. XPC—comparison of individual strands—ScdA Cytoplasmic Extract, Figure S11: Endonucleolytic activity of xrs5 vs. BJ vs. XPC—comparison of individual strands—RcdA Cytoplasmic Extract, Figure S12: Polymerase activity of xrs5 vs. BJ vs. XPC—comparison of individual strands—ScdA Cytoplasmic Extract, Figure S13: Polymerase activity of xrs5 vs. BJ vs. XPC—comparison of individual strands—RcdA Cytoplasmic Extract, Figure S14: Exonucleolytic activity of xrs5 vs. BJ vs. XPC—comparison of individual strands—ScdA Cytoplasmic Extract, Figure S15: Exonucleolytic activity of xrs5 vs. BJ vs. XPC—comparison of individual strands—RcdA Cytoplasmic Extract. Table S1: The full sequence list of substrate oligonucleotides, Table S2: The masses (calculated vs. found) of chosen substrate oligos, Table S3: Xrs5—Control 1. Raw numerical data of densitometry, Table S4: BJ—Control 1. Raw numerical data of densitometry, Table S5: XPC—Control 1. Raw numerical data of densitometry, Table S6: Xrs5—ScdA. Raw numerical data of densitometry, Table S7: Xrs5—RcdA. Raw numerical data of densitometry, Table S8: BJ—ScdA. Raw numerical data of densitometry, Table S9: BJ—RcdA. Raw numerical data of densitometry, Table S10: XPC—ScdA. Raw numerical data of densitometry, Table S11: XPC—RcdA. Raw numerical data of densitometry.

Author Contributions: Conceptualization and methodology B.T.K.; validation, K.B., J.K.-B. and B.T.K.; formal analysis, K.B. and B.T.K.; investigation, K.B. and J.K.-B.; resources, J.K.-B. and B.T.K.; data curation, K.B.; writing—original draft preparation, K.B.; writing—review and editing, K.B., J.K.-B. and B.T.K.; visualization, K.B.; supervision, B.T.K.; project administration, B.T.K.; funding acquisition, B.T.K. All authors have read and agreed to the published version of the manuscript.

Funding: This research was funded by the National Science Center, Poland (grant No. 2016/23/B/NZ7/03367).

Institutional Review Board Statement: Not applicable.

Informed Consent Statement: Not applicable.

Data Availability Statement: Not applicable.

Conflicts of Interest: The authors declare no conflict of interest.

References

1. Bayley, S.T. Autoradiography of Single Cells. *Nature* **1947**, *160*, 193–194. [CrossRef]
2. Eccles, L.J.; Lomax, M.E.; O'Neill, P. Hierarchy of Lesion Processing Governs the Repair, Double-Strand Break Formation and Mutability of Three-Lesion Clustered DNA Damage. *Nucleic Acids Res.* **2009**, *38*, 1123–1134. [CrossRef]
3. Mourgues, S.; Lomax, M.E.; O'Neill, P. Base Excision Repair Processing of Abasic Site/Single-Strand Break Lesions within Clustered Damage Sites Associated with XRCC1 Deficiency. *Nucleic Acids Res.* **2007**, *35*, 7676–7687. [CrossRef]
4. Lomax, M.E.; Cunniffe, S.; O'Neill, P. Efficiency of Repair of an Abasic Site within DNA Clustered Damage Sites by Mammalian Cell Nuclear Extracts. *Biochemistry* **2004**, *43*, 11017–11026. [CrossRef]

5. Eccles, L.J.; Menoni, H.; Angelov, D.; Lomax, M.E.; O'Neill, P. Efficient Cleavage of Single and Clustered AP Site Lesions within Mono-Nucleosome Templates by CHO-K1 Nuclear Extract Contrasts with Retardation of Incision by Purified APE1. *DNA Repair* **2015**, *35*, 27–36. [CrossRef]
6. Karwowski, B.T. (5′*S*) 5′,8-Cyclo-2′-Deoxyadenosine Cannot Stop BER. Clustered DNA Lesion Studies. *Int. J. Mol. Sci.* **2021**, *22*, 5934. [CrossRef]
7. Boguszewska, K.; Kaźmierczak-Barańska, J.; Karwowski, B.T. The Influence of 5′,8-Cyclo-2′-Deoxypurines on the Mitochondrial Repair of Clustered Dna Damage in Xrs5 Cells: The Preliminary Study. *Molecules* **2021**, *26*, 7042. [CrossRef]
8. Boguszewska, K.; Szewczuk, M.; Kaźmierczak-Barańska, J.; Karwowski, B.T. How (5′*S*) and (5′*R*) 5′,8-Cyclo-2′-Deoxypurines Affect Base Excision Repair of Clustered DNA Damage in Nuclear Extracts of Xrs5 Cells? A Biochemical Study. *Cells* **2021**, *10*, 725. [CrossRef]
9. Karwowski, B.; Czarny, P.; Szemraj, J.; Śliwiński, T.; Majchrzak, K.; Merecz-Sadowska, A.; Jabłkowski, M. The Influence of Hepatitis C Virus Therapy on the DNA Base Excision Repair System of Peripheral Blood Mononuclear Cells. *DNA Cell Biol.* **2017**, *36*, 535–540. [CrossRef]
10. Karwowski, B.T.; Bellon, S.; O'Neill, P.; Lomax, M.E.; Cadet, J. Effects of (5′*S*)-5′,8-Cyclo-2′-Deoxyadenosine on the Base Excision Repair of Oxidatively Generated Clustered DNA Damage. A Biochemical and Theoretical Study. *Org. Biomol. Chem.* **2014**, *12*, 8671–8682. [CrossRef]
11. Bundy, D. Autoradiography. In *Current Protocols in Protein Science*; John Wiley & Sons Inc.: Hoboken, NJ, USA, 1997; pp. 10.11.1–10.11.6.
12. Voytas, D.; Ke, N. Detection and Quantitation of Radiolabeled Proteins and DNA in Gels and Blots. In *Current Protocols in Immunology*; John Wiley & Sons Inc.: Hoboken, NJ, USA, 2002; pp. A.31.1–A.31.10.
13. Lomax, M.E.; Folkes, L.K.; O'Neill, P. Biological Consequences of Radiation-Induced DNA Damage: Relevance to Radiotherapy. *Clin. Oncol.* **2013**, *25*, 578–585. [CrossRef] [PubMed]
14. Burkart, W.; Jung, T.; Frash, G. Damage Pattern as a Function of Radiation Quality and Other Factors. *Comptes Rendus l'Académie Sci.* **1999**, *322*, 89–101. [CrossRef]
15. Cadet, J.; Ravanat, J.-L.; TavernaPorro, M.; Menoni, H.; Angelov, D. Oxidatively Generated Complex DNA Damage: Tandem and Clustered Lesions. *Cancer Lett.* **2012**, *327*, 5–15. [CrossRef] [PubMed]
16. Karwowski, B.T. The Influence of Single, Tandem, and Clustered DNA Damage on the Electronic Properties of the Double Helix: A Theoretical Study. *Molecules* **2020**, *25*, 3126. [CrossRef]
17. Chatgilialoglu, C.; Ferreri, C.; Geacintov, N.E.; Krokidis, M.G.; Liu, Y.; Masi, A.; Shafirovich, V.; Terzidis, M.A.; Tsegay, P.S. 5′,8-Cyclopurine Lesions in DNA Damage: Chemical, Analytical, Biological, and Diagnostic Significance. *Cells* **2019**, *8*, 513. [CrossRef]
18. Pande, P.; Das, R.S.; Sheppard, C.; Kow, Y.W.; Basu, A.K. Repair Efficiency of (5′*S*)-8,5′-Cyclo-2′-Deoxyguanosine and (5′*S*)-8,5′-Cyclo-2′-Deoxyadenosine Depends on the Complementary Base. *DNA Repair* **2012**, *11*, 926–931. [CrossRef]
19. Karwowski, B.T. The Influence of (5′*R*)- and (5′*S*)-5′,8-Cyclo-2′-Deoxyadenosine on UDG and HAPE1 Activity. Tandem Lesions Are the Base Excision Repair System's Nightmare. *Cells* **2019**, *8*, 1303. [CrossRef]
20. Jaruga, P.; Rozalski, R.; Jawien, A.; Migdalski, A.; Olinski, R.; Dizdaroglu, M. DNA Damage Products (5′*R*)- and (5′*S*)-8,5′-Cyclo-2′-Deoxyadenosines as Potential Biomarkers in Human Urine for Atherosclerosis. *Biochemistry* **2012**, *51*, 1822–1824. [CrossRef]
21. Mori, T.; Nakane, H.; Iwamoto, T.; Krokidis, M.G.; Chatgilialoglu, C.; Tanaka, K.; Kaidoh, T.; Hasegawa, M.; Sugiura, S. High Levels of Oxidatively Generated DNA Damage 8,5′-Cyclo-2′-Deoxyadenosine Accumulate in the Brain Tissues of Xeroderma Pigmentosum Group A Gene-Knockout Mice. *DNA Repair* **2019**, *80*, 52–58. [CrossRef]
22. Jaruga, P.; Theruvathu, J.; Dizdaroglu, M.; Brooks, P.J. Complete Release of (5′*S*)-8,5′-Cyclo-2′-Deoxyadenosine from Dinucleotides, Oligodeoxynucleotides and DNA, and Direct Comparison of Its Levels in Cellular DNA with Other Oxidatively Induced DNA Lesions. *Nucleic Acids Res.* **2004**, *32*, e87. [CrossRef]
23. Pednekar, V.; Weerasooriya, S.; Jasti, V.P.; Basu, A.K. Mutagenicity and Genotoxicity of (5′*S*)-8,5′-Cyclo-2′-Deoxyadenosine in *Escherichia coli* and Replication of (5′*S*)-8,5′-Cyclopurine-2′-Deoxynucleosides in Vitro by Dna Polymerase Iv, Exo-Free Klenow Fragment, and Dpo4. *Chem. Res. Toxicol.* **2014**, *27*, 200–210. [CrossRef] [PubMed]
24. Jaruga, P.; Birincioglu, M.; Rodriguez, H.; Dizdaroglu, M. Mass Spectrometric Assays for the Tandem Lesion 8,5′-Cyclo-2′-Deoxyguanosine in Mammalian DNA. *Biochemistry* **2002**, *41*, 3703–3711. [CrossRef] [PubMed]
25. Kuraoka, I.; Bender, C.; Romieu, A.; Cadet, J.; Wood, R.D.; Lindahl, T. Removal of Oxygen Free-Radical-Induced 5′,8-Purine Cyclodeoxynucleosides from DNA by the Nucleotide Excision-Repair Pathway in Human Cells. *Proc. Natl. Acad. Sci. USA* **2000**, *97*, 3832–3837. [CrossRef]
26. Bukowska, B.; Karwowski, B.T. The Clustered DNA Lesions—Types, Pathways of Repair and Relevance to Human Health. *Curr. Med. Chem.* **2018**, *25*, 2722–2735. [CrossRef] [PubMed]
27. Brooks, P.J. The Cyclopurine Deoxynucleosides: DNA Repair, Biological Effects, Mechanistic Insights, and Unanswered Questions. *Free Radic. Biol. Med.* **2017**, *107*, 90–100. [CrossRef] [PubMed]
28. David-Cordonnier, M.H.; Cunniffe, S.M.T.; Hickson, I.D.; O'Neill, P. Efficiency of Incision of an AP Site within Clustered DNA Damage by the Major Human AP Endonuclease. *Biochemistry* **2002**, *41*, 634–642. [CrossRef] [PubMed]

29. Merecz, A.; Karwowski, B.T. DNA Tandem Lesion: 5′,8-Cyclo-2′-Deoxyadenosine. The Influence on Human Health. *Mol. Biol.* **2016**, *50*, 793–798. [CrossRef]
30. Kaźmierczak-Barańska, J.; Boguszewska, K.; Szewczuk, M.; Karwowski, B.T. Effects of 5′,8′-Cyclo-2′-Deoxypurines on the Base Excisionrepair of Clustered DNA Lesions in Nuclear Extracts of the Xpc Cell Line. *Cells* **2021**, *10*, 3254. [CrossRef]
31. Szewczuk, M.; Boguszewska, K.; Kaźmierczak-Barańska, J.; Karwowski, B.T. The Influence of 5′*R* and 5′*S* Cda and Cdg on the Activity of Bsmai and Sspi Restriction Enzymes. *Molecules* **2021**, *26*, 3750. [CrossRef]
32. Szewczuk, M.; Boguszewska, K.; Kaźmierczak-Barańska, J.; Karwowski, B.T. When Udg and Hape1 Meet Cyclopurines. How (5′*R*) and (5′*S*) 5′,8-Cyclo-2′-Deoxyadenosine and 5′,8-Cyclo-2′-Deoxyguanosine Affect Udg and Hape1 Activity? *Molecules* **2021**, *26*, 5177. [CrossRef]
33. Szewczuk, M.; Karwowski, B. The Influence of CdG on 8-OxodG Excision by OGG1 and FPG Glycosylases. *Acta Biochim. Pol.* **2022**, *69*, 227–232. [CrossRef]
34. Jaruga, P.; Dizdaroglu, M. 8,5′-Cyclopurine-2′-Deoxynucleosides in DNA: Mechanisms of Formation, Measurement, Repair and Biological Effects. *DNA Repair* **2008**, *7*, 1413–1425. [CrossRef] [PubMed]
35. Brooks, P.J. The 8,5′-Cyclopurine-2′-Deoxynucleosides: Candidate Neurodegenerative DNA Lesions in Xeroderma Pigmentosum, and Unique Probes of Transcription and Nucleotide Excision Repair. *DNA Repair* **2008**, *7*, 1168–1179. [CrossRef] [PubMed]
36. Kraemer, K.H.; Patronas, N.J.; Schiffmann, R.; Brooks, B.P.; Tamura, D.; DiGiovanna, J.J. Xeroderma Pigmentosum, Trichodystrophy and Cockayne Syndrome: A Complex Genotype-Phenotype Relationship. *Neuroscience* **2007**, *145*, 1388–1396. [CrossRef] [PubMed]
37. Fayyad, N.; Kobaisi, F.; Beal, D.; Mahfouf, W.; Ged, C.; Morice-Picard, F.; Fayyad-Kazan, M.; Fayyad-Kazan, H.; Badran, B.; Rezvani, H.R.; et al. Xeroderma Pigmentosum C (XPC) Mutations in Primary Fibroblasts Impair Base Excision Repair Pathway and Increase Oxidative DNA Damage. *Front. Genet.* **2020**, *11*, 1458. [CrossRef]
38. Shivji, M.K.K.; Eker, A.P.M.; Wood, R.D. DNA Repair Defect in Xeroderma Pigmentosum Group C and Complementing Factor from HeLa Cells. *J. Biol. Chem.* **1994**, *269*, 22749–22757. [CrossRef]
39. Gong, L.; Zhang, Y.; Liu, C.; Zhang, M.; Han, S. Application of Radiosensitizers in Cancer Radiotherapy. *Int. J. Nanomed.* **2021**, *16*, 1083–1102. [CrossRef]
40. Herath, N.I.; Berthault, N.; Thierry, S.; Jdey, W.; Lienafa, M.C.; Bono, F.; Noguiez-Hellin, P.; Sun, J.S.; Dutreix, M. Preclinical Studies Comparing Efficacy and Toxicity of DNA Repair Inhibitors, Olaparib, and AsiDNA, in the Treatment of Carboplatin-Resistant Tumors. *Front. Oncol.* **2019**, *9*, 1097. [CrossRef]
41. Jdey, W.; Thierry, S.; Russo, C.; Devun, F.; Al Abo, M.; Noguiez-Hellin, P.; Sun, J.S.; Barillot, E.; Zinovyev, A.; Kuperstein, I.; et al. Drug-Driven Synthetic Lethality: Bypassing Tumor Cell Genetics with a Combination of AsiDNA and PARP Inhibitors. *Clin. Cancer Res.* **2017**, *23*, 1001–1011. [CrossRef]
42. Gökirmak, T.; Nikan, M.; Wiechmann, S.; Prakash, T.P.; Tanowitz, M.; Seth, P.P. Overcoming the Challenges of Tissue Delivery for Oligonucleotide Therapeutics. *Trends Pharmacol. Sci.* **2021**, *42*, 588–604. [CrossRef]
43. Hammond, S.M.; Aartsma-Rus, A.; Alves, S.; Borgos, S.E.; Buijsen, R.A.M.; Collin, R.W.J.; Covello, G.; Denti, M.A.; Desviat, L.R.; Echevarría, L.; et al. Delivery of Oligonucleotide-based Therapeutics: Challenges and Opportunities. *EMBO Mol. Med.* **2021**, *13*, e13243. [CrossRef] [PubMed]
44. Ferreira, S.; Foray, C.; Gatto, A.; Larcher, M.; Heinrich, S.; Lupu, M.; Mispelter, J.; Boussin, F.D.; Pouponnot, C.; Dutreix, M. AsiDNA Is a Radiosensitizer with No Added Toxicity in Medulloblastoma Pediatric Models. *Clin. Cancer Res.* **2021**, *26*, 5735–5746. [CrossRef] [PubMed]
45. Johannes, L.; Lucchino, M. Current Challenges in Delivery and Cytosolic Translocation of Therapeutic RNAs. *Nucleic Acid Ther.* **2018**, *28*, 178–193. [CrossRef] [PubMed]
46. Topf, U.; Wrobel, L.; Chacinska, A. Chatty Mitochondria: Keeping Balance in Cellular Protein Homeostasis. *Trends Cell Biol.* **2016**, *26*, 577–586. [CrossRef] [PubMed]
47. Chacinska, A.; Rehling, P. Moving Proteins from the Cytosol Intomitochondria. *Biochem. Soc. Trans.* **2004**, *32*, 774–776. [CrossRef] [PubMed]
48. Karwowski, B.T.; Grand, A.; Cadet, J. 5′,8-Cyclo-2′-Deoxyadenosine (CdA) Formation by γ-Radiation. Theoretical Quantum Mechanics Study. *Acta Biochim. Pol.* **2009**, *56*, 655–662. [CrossRef]
49. Karwowski, B.T. Formation of 5′,8-Cyclo-2′-Deoxyadenosine in Single Strand DNA. Theoretical Quantum Mechanics Study. *Org. Biomol. Chem.* **2010**, *8*, 1603. [CrossRef]
50. Guerrero, C.R.; Wang, J.; Wang, Y. Induction of 8,5′-Cyclo-2′-Deoxyadenosine and 8,5′-Cyclo-2′-Deoxyguanosine in Isolated DNA by Fenton-Type Reagents. *Chem. Res. Toxicol.* **2013**, *26*, 1361–1366. [CrossRef]
51. Kaniak-Golik, A.; Skoneczna, A. Mitochondria-Nucleus Network for Genome Stability. *Free. Radic. Biol. Med.* **2015**, *82*, 73–104. [CrossRef]
52. Shaughnessy, D.T.; McAllister, K.; Worth, L.; Haugen, A.C.; Meyer, J.N.; Domann, F.E.; van Houten, B.; Mostoslavsky, R.; Bultman, S.J.; Baccarelli, A.A.; et al. Mitochondria, Energetics, Epigenetics, and Cellular Responses to Stress. *Environ. Health Perspect.* **2015**, *122*, 1271–1278. [CrossRef]
53. Izumi, T.; Mellon, I. *Base Excision Repair and Nucleotide Excision Repair*; Elsevier Inc.: Amsterdam, The Netherlands, 2016; ISBN 9780128033456.
54. Prakash, A.; Doublie, S. Base Excision Repair in the Mitochondria. *J. Cell Biochem.* **2015**, *116*, 1490–1499. [CrossRef] [PubMed]

55. Frosina, G.; Fortini, P.; Rossi, O.; Carrozzino, F.; Raspaglio, G.; Cox, L.S.; Lane, D.P.; Abbondandolo, A.; Dogliotti, E. Two Pathways for Base Excision Repair in Mammalian Cells. *J. Biol. Chem.* **1996**, *271*, 9573–9578. [CrossRef] [PubMed]
56. Romieu, A.; Gasparutto, D.; Cadet, J. Synthesis and Characterization of Oligonucleotides Containing 5′,8- Cyclopurine 2′-Deoxyribonucleosides: (5′*R*)-5′,8-Cyclo-2′-Deoxyadenosine, (5′*S*)-5′,8-Cyclo-2′-Deoxyguanosine, and (5′*R*)-5′,8-Cyclo-2′-Deoxyguanosine. *Chem. Res. Toxicol.* **1999**, *12*, 412–421. [CrossRef] [PubMed]
57. Walker, G.; Chatterjee, N. Mechanisms of DNA Damage, Repair, and Mutagenesis. *Environ. Mol. Mutagenesis* **2017**, *58*, 235–263. [CrossRef]
58. Vilenchik, M.M.; Knudson, A.G. Endogenous DNA Double-Strand Breaks: Production, Fidelity of Repair, and Induction of Cancer. *Proc. Natl. Acad. Sci. USA* **2003**, *100*, 12871–12876. [CrossRef]
59. Tubbs, A.; Nussenzweig, A. Endogenous DNA Damage as a Source of Genomic Instability in Cancer. *Cell* **2017**, *168*, 644–656. [CrossRef]
60. Jang, B.; Kwon, H.; Katila, P.; Lee, S.J.; Lee, H. Dual Delivery of Biological Therapeutics for Multimodal and Synergistic Cancer Therapies. *Adv. Drug Deliv. Rev.* **2016**, *98*, 113–133. [CrossRef]
61. Takakura, K.; Kawamura, A.; Torisu, Y.; Koido, S.; Yahagi, N.; Saruta, M. The Clinical Potential of Oligonucleotide Therapeutics against Pancreatic Cancer. *Int. J. Mol. Sci.* **2019**, *20*, 3331. [CrossRef]
62. Lundin, K.E.; Gissberg, O.; Smith, C.I.E. Oligonucleotide Therapies: The Past and the Present. *Hum. Gene Ther.* **2015**, *26*, 475–485. [CrossRef]
63. Roberts, T.C.; Langer, R.; Wood, M.J.A. Advances in Oligonucleotide Drug Delivery. *Nat. Rev. Drug Discov.* **2020**, *19*, 673–694. [CrossRef]
64. Jasti, V.P.; Das, R.S.; Hilton, B.A.; Weerasooriya, S.; Zou, Y.; Basu, A.K. (5′*S*)-8,5′-Cyclo-2′-Deoxyguanosine Is a Strong Block to Replication, a Potent Pol V-Dependent Mutagenic Lesion, and Is Inefficiently Repaired in *Escherichia coli*. *Biochemistry* **2011**, *50*, 3862–3865. [CrossRef] [PubMed]
65. Krokan, H.E.; Bjørås, M. Base Excision Repair. *Cold Spring Harb. Perspect. Biol.* **2013**, *5*, a012583. [CrossRef] [PubMed]